www.czasopisma.pan.pl PAN POLSKA AKADEMIA NAUK www.journals.pan.pl

Archives of Acoustics Vol. **48**, No. 1, pp. 141–148 (2023), doi: 10.24425/aoa.2023.144268

Research Paper

Non-invasive Ultrasound Doppler Effect Based Method of Liquid Flow Velocity Estimation in Pipe

Pawel BIERNACKI*, Stanislaw GMYREK, Wladyslaw MAGIERA

Faculty of Electronics, Photonics and Microsystems, Department of Acoustics, Multimedia and Signal Processing
Wroclaw University of Science and Technology
Wrocław, Poland

*Corresponding Author e-mail: pawel.biernacki@pwr.edu.pl

(*received June 8, 2022; accepted November 7, 2022*)

This paper discusses the estimation of flow velocity from a multi-sensor scenario. Different estimation methods were used, which allow the effective measurement of the actual Doppler shift in a noisy environment, such as water with air bubbles, and on this basis the estimation of the flow velocity in the pipe was calculated. Information fusion is proposed for the estimates collected. The proposed approach focuses on the density of the fluid. The proposed method is capable of determining the flow velocity with high accuracy and small variations. Simulation results for plastic and steel (both galvanized and non-galvanized) pipes show the possibility of accurate fluid flow measurements without the need for sensors inside the pipe.

Keywords: information fusion; flow velocity; Doppler effect.

1. Introduction

Calm-on flowmeters are becoming increasingly popular. Their main advantage is fast and non-invasive installation. They can be used as portable devices in applications such as channel infiltration capacity testing, delivery control, consumption verification, measurement campaigns. Direct and indirect approaches can be distinguished (Raffel *et al.*, 1998). Direct methods typically involve probes that are placed directly in the fluid drift. On the other hand, indirect methods do not disturb fluid flow and consist of particle image velocimetry (PIV) (Atkins, 2016; Kaipio *et al.*, 2017) and laser Doppler anemometry (LDA) (Solero, Beghi, 1995; Doran, 2013).

Methods based on digital signal processing are becoming more and more popular. The cross-correlation method is to look for the time delay of the flow structure passing from upstream sensors to downstream sensors (Beck, Plaskowski, 1987; Lucas *et al.*, 1999). The pixel-based cross-correlation solution can reconstruct the radial velocity distribution (Cui *et al.*, 2016; Xu *et al.*, 2009). The ability of acoustic transducers to characterize underwater dynamic phenomena may be used in non-invasive measurement scenarios (Cochran, 2001; Jones, 1995; Buermans *et al.*, 2009). In medical echography, the Doppler signal analysis is one of the most vital diagnostic techniques (Matani *et al.*, 1996).

There are four basic measurement methods based on:

1) estimation of the time of a sine wave propagation in the tube (transit-time flow) (Takeda, 2012),
2) using the Doppler effect for the emitted sinusoidal wave (pulsed Doppler flow) (Mori *et al.*, 2004; Wu, 2018),
3) measuring of ultrasonic wave lift (Kang *et al.*, 2019),
4) correlation method (Avilán *et al.*, 2013).

The operation of the transit flow involves sending and receiving ultrasound pulses through a pair of probes and measuring the difference in signal transit time. The probes used are mounted outside the pipe, generating pulses that pass through the wall of the pipe. The liquid flowing in the pipeline creates a difference in the signal beam transit time. This time is

measured by a flowmeter, and the flow rate is then calculated. The key principle of the method is that sound waves traveling in the direction of the liquid have a higher speed than those traveling in the opposite direction. The difference in the signal transit time is proportional to the liquid flow rate. It is shown in Fig. 1 and can be written as:

$$V_{\text{liquid}} = \frac{\Delta t c^2_{\text{liquid}}}{2L\cos\theta} = \frac{\Delta t c^2_{\text{liquid}}}{2L\sin\alpha}. \tag{1}$$

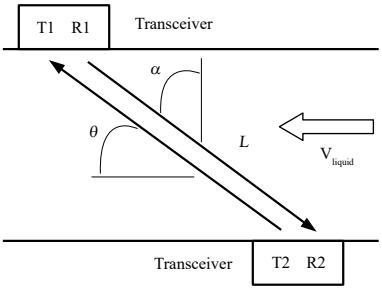

Fig. 1. Time transit measurement method of liquid flow velocity.

The time-of-flight flow measurement technology can provide reliable performance over a wide range of fluid flow conditions, but there are cases where a high percentage of undissolved gases or solids can scatter the acoustic beam and prevent the appropriate signal amplitude from reaching the receiving transducer (Takeda, 1995). Under such conditions, a Doppler measurement may be required to meet the customer's flow measurement needs.

The method of ultrasonic wave lift is based on shifting the point of incidence of the wave along the pipeline, in proportion to the average speed of the fluid), with:

$$V_{\text{liquid}} \propto (A_1 - A_2), \tag{2}$$

where A_1 and A_2 are the amplitudes of the ultrasonic waves received by the receivers R_1 and R_2. As the velocity of the fluid increases, the signal in the receiver R_1 decreases and in the receiver R_2 increases, and the difference in signal amplitudes carries information about the fluid velocity. This approach is shown in Fig. 2.

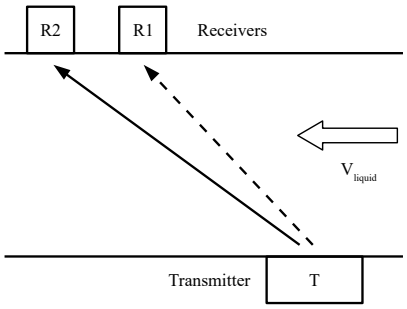

Fig. 2. Wave lift measurement method of liquid flow velocity.

The correlation method (Fig. 3) of measurement based on the time shift of the receiving signals for which there is a maximum of cross-correlation. Such a sensor can also be used for vortex frequency and thermal disturbance detections.

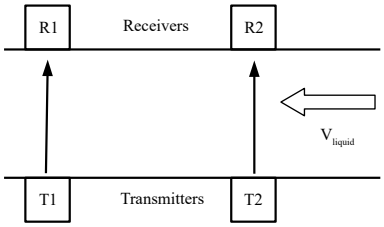

Fig. 3. Correlation measurement method of the flow velocity of liquid.

The pulse Doppler method appears to be the latest and most accurate way to measure the flow of liquids containing large amounts of undissolved gases or suspended solids (Lucas *et al.*, 1999). This method uses the Doppler phenomenon to measure the frequency difference of a continuous signal transmitted and received in a liquid with reflective elements (e.g., air bubbles). Its method of operation is described in the next section. It is possible to develop the pulsed Doppler method that automatically switches from time-of-flight to the Doppler measurement without changing the transducer position, suggesting the use of the transceiver method. In the minimum hardware version, this solution requires only one transceiver that acts as a transmitter and a receiver interchangeably. It is shown in Fig. 4. Ultrasonic liquid flow velocity methods have the following advantages:

- No moving parts: traditional mechanical flowmeters measure pressure through the use of moving parts that serve as mechanical sensors. Because there are no moving parts on ultrasonic flowmeters, one does not have to worry about them degrading or creating a blockage.
- Low maintenance: because ultrasonic flowmeters do not involve moving parts, they last a long time and need very little maintenance. They also have low power consumption, so they often last several years before the batteries are to be replaced.
- High accuracy: as long as the meter is properly mounted and installed, these meters are highly accurate. However, inline and insertion flowmeters

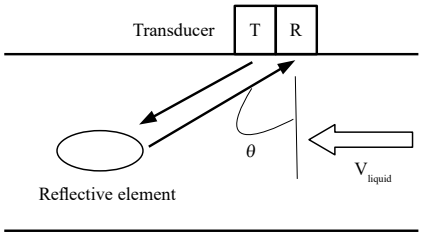

Fig. 4. Doppler measurement method of liquid flow velocity.

are generally more accurate than clamp-on ultrasonic flowmeters.
- Bi-directional measurements: although many traditional flowmeters only measure in a single direction, transit-time ultrasonic flowmeters measure flow in both directions, forward, and reverse.
- High stability: transit-time meters are unaffected by the temperature, density, or concentration of the liquids they measure, making them a more stable measuring device. Ability to measure liquids and gases. Ultrasonic flowmeters can be used to measure a wide variety of liquids.

The disadvantages include:
- Sensitivity to temperature changes: Doppler-type ultrasonic transducers are sensitive to changes in temperature, density, and concentration, meaning that any changes to the contents of the pipe may negatively affect the accuracy of the Doppler transducer results.
- Substance limitations: working with slurries where the flow is not linear may produce measurement errors.

The organization of the paper is as follows: in Secs. 2 and 3 we discuss the methodology for estimating the liquid flow velocity. Sections 4, 5, and 6 include mathematical tools used for measuring system. Section 7 describes some simulations performed in the real-life working system. The paper ends with some conclusions and suggestions for the next steps in increasing the accuracy of the measurement.

2. Metodology of measurements

In single-sensor detection, the signal is subjected to individual preprocessing and then different Doppler shift estimation methods are used. The environment is characterized by a high level of noise (especially in steel pipes), which leads to false results that are indistinguishable from the true values. When using multiple sensors, the actual fluid velocity is obtained by comparing the results from individual sensors using different methods. The decision is obtained from a joint density of the results taking into account the results from all sensors. A joint density for as few as two sensors gives significantly better speed detection than using only one sensor. We compare the use of individual parameterisation methods to the case of multisensor data fusion at the decision level. The results acquired from the individual sensors are used to estimate the Doppler shift; we estimate the probability density function of the fluid flow velocity.

3. Doppler shift and velocity flow equation

We have the continuous-wave Doppler system. In this case, two transducers are used: the first transducer transmits an acoustic signal into the fluid, while the second transducer is used to receive the reflected signal. Reflections come from the scattering particles within the fluid. The Doppler shift frequency depends on the fluid velocity. This affects the reflected signal, which is an expanded (or compressed) version of the transmitted signal. The difference between them gives us the Doppler shift frequency. In the standard approach, the Doppler flow equation also takes into account the fluid sound speed as well as the beam angle in the fluid. In our case, we do not need these two parameters. It would be redundant because using the refractive clamp-on transducer implies that the sine of the beam angle and the sound speed are constant.

We have the Doppler shift frequency:

$$\Delta f = 2f\sin(\theta)\frac{v}{c}. \tag{3}$$

From

$$Tr_{\text{phase}} = \frac{c}{\sin(\theta)} \tag{4}$$

we have

$$\Delta f = 2f\frac{v}{Tr_{\text{phase}}}. \tag{5}$$

It results in a form:

$$v = Tr_{\text{phase}}\frac{\Delta f}{2f}, \tag{6}$$

where V_{phase} is the transducer phase parameter that depends on the angle of the transmitted wave, f is the transmit frequency, Δf is the Doppler shift frequency, v is the flow velocity, c is the sound velocity in the liquid.

4. Extended Kalman filter

To adapt the Kalman filter to nonlinear optimal filtering problems, the Extended Kalman Filter (EKF) (Jazwinski, 1970; Maybeck, 1982; Bar-Shalom *et al.*, 2004; Grewal, Andrews, 2001; Särkkä, 2006) is used. It requires determining a Gaussian approximation to the joint distribution of state x and measurements y (with Taylor series-based transformation involved):

$$x_k = f(x_{k-1}, k-1) + q_{k-1}, \tag{7}$$

$$y_k = h(x_k, k) + r_k, \tag{8}$$

where x_k is the state, y_k is the measurement, q_{k-1} is the process noise, r_k is the measurement noise, f is the dynamic model function, h is the measurement model function. The state vector (in the sine wave case) may be written as:

$$x_k = (\theta_k, \omega_k, a_k), \tag{9}$$

where θ_k is the parameter for the sine function on the time step k, $\frac{\mathrm{d}\theta}{\mathrm{d}t} = \omega$, ω_k is the angular velocities in time

step k, a_k is the amplitude in the time step k. The dynamic equation in the discretized form is:

$$x_k = \begin{pmatrix} 1 & \Delta t & 0 \\ 0 & 1 & 0 \\ 0 & 0 & 1 \end{pmatrix}. \tag{10}$$

The measurement function $h(x_k, k)$, given by

$$h(x_k, k) = a_k \sin(\theta_k), \tag{11}$$

is a sine function. The measurement model as follows:

$$y_k = h(x_k, k) + r_k, \tag{12}$$

where r_k is the white Gaussian noise with zero mean and variance 1.

5. Power spectral density estimation

Power spectral density (PSD) estimation techniques can be divided into parametric and non-parametric methods. Non-parametric methods estimate PSD explicitly from signal samples, without making any assumptions about the particular process structure. Parametric approaches assume that signal can be described as the stationary process (MA, AR, or ARMA) of order p. The power spetral density is then calculated using estimated model parameters. This paper presents PSD estimated with parametric approaches (Burg and Prony's method) and non-parametric methods (Welch's and Thomson multitaper method). On the basis of the signal spectrum, it is possible to determine the dominant frequency (weighted average), which estimates the Doppler shift, Δf.

5.1. The Burg algorithm

The Burg algorithm assumes that the signal can be described as the AR process of order p:

$$\widehat{x} = -\sum_{k=1}^{m} a_m(k) x(n-k). \tag{13}$$

There are many techniques for estimating the a_m parameters such as the Yule-Walker algorithm, or least squares estimator (Kaipio *et al.*, 2015). The Burg algorithm solves the ordinary least-squares problem. The AR parameters a_m are estimated by minimizing the prediction forward and backward errors, which are referred to as the error between the actual value signal and the corresponding estimators forward and backward (Atkins, 2016):

$$\mathrm{PSD}x(f) = \frac{E_m}{\left|1 + \sum_{k=1}^{m} a(k) e^{-j2\pi fk}\right|^2}. \tag{14}$$

The results obtained by the Burg algorithm have a high frequency resolution (Atkins, 2016), and are more objective and stable than the other algorithms for estimating the power spectral density using the AR model.

5.2. The Prony algorithm

Prony proposed that the N data samples can be approximated using the sum of complex, damped exponentials:

$$\widehat{x}(k) = \sum_{i=0}^{p} a_i \cdot z_i^k, \qquad k = 0, ..., N-1, \tag{15}$$

with $a_i = A_i \cdot e^{j\theta_i}$, $z_i = e^{\alpha_i + 2\pi j f T}$, where T is the period, A_i, α_i, f_i, θ_i are the amplitude, damping factor, frequency and initial phase of the complex, dumped exponentials. The fitness problem leads to a minimization error between the data $x(n)$ and the fitted value $\widehat{x}(n)$. The complicated nonlinear problem, with the Prony method, can be converted to the linear prediction problem, and $x(n)$ can be regraded as the output of the p-th order of AR process. The PSD is given by:

$$\mathrm{PSD}x(f) = \left| \sum_{i=1}^{p} A_i \cdot e^{j\theta_i} \frac{2\alpha_i}{(\alpha_i^2 + (2\pi(f - fi))^2)} \right|^2. \tag{16}$$

The Prony method provides greater accuracy and does not have a problem with spectral leakage.

5.3. The Welch algorithm

To estimate PSD with the Welch method, the signal should be divided into overlapping segments and multiplied by a window function. Then, for each part of the signal, the modified periodogram is computed. The power spectral density is estimated by averaging the periodograms. The estimate is given by:

$$\mathrm{PSD}x(f) = \frac{1}{M} \sum_{m=1}^{M} \left\{ \frac{2}{N_f} \left| \sum_{n=0}^{N-1} x(n+mD) e^{-j2\pi nk} \right|^2 \right\}, \tag{17}$$

where M denotes the number of signal fragments of length N_f and D denotes delay. The Welch method reduces the variance of the classic periodogram (Lyons, 2004).

5.4. Multitaper PSD estimate

Power spectral density estimate computed using the multitaper method utilizes mutually orthogonal windows – discrete prolate spheroidal (Slepian) sequences:

$$\mathrm{PSD}x^{MT}(f) = \frac{1}{L} \sum_{l=0}^{L-1} \mathrm{PSD}x_l(f), \tag{18}$$

where

$$\mathrm{PSD}x_l(f) = \Delta t \left| \sum_{n=0}^{N-1} s_l(n) x(n) e^{-j2\pi f_n \Delta t} \right| \tag{19}$$

can be considered as the modified periodogram computed with the l-th Slepian sequence $s_l(n)$. The multitaper PSD estimate averages the L periodograms.

The multitaper method (MTM) is similar to the Welch estimators, but in this approach, the periodograms are decorelated due to the orthogonality of Slepian sequences. The Welch approach computes the modified periodograms using the overlapping segments of the signal, whereas the MTM method uses the entire signal to compute the modified periodogram. The examples of the first five Slepian sequences are presented in Fig. 5.

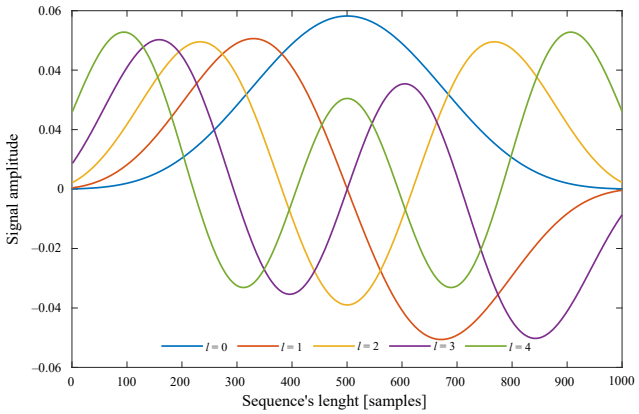

Fig. 5. Examples of five Slepian sequences used in MTM method.

6. Kernel density estimation

In order to estimate a probability density function $\widehat{f}(x)$ we need to use a statistical method using a set of samples $x_1, ..., x_n$. For this we use kernel density estimation (KDE). In each step, the i-th sample x_i is assigned to a kernel function $K(x,t)$:

$$\widehat{f} = \frac{1}{n}\sum_{i=1}^{n} K(x_i, t). \tag{20}$$

In the special case we have a form:

$$K_{\text{sym}}(x,t) = \frac{1}{h}K\left(\frac{x-t}{h}\right), \tag{21}$$

which is valid when our kernel is symmetric. In Eq. (21) h represents the smoothing parameter or bandwidth. Control the smoothing factor for each sample. It is very important to choose the right value for h. Taking a wrong value, too small or too large, will affect the estimator. There are insignificant details shown when h is too small. On the other hand, the estimated probability density function will be too smooth and the information from the sample may be lost.

In our proposal, we use the bivariate extension:

$$\widehat{f}(x,y) = \frac{1}{nh_xh_y}\sum_{i=1}^{n} K\left(\frac{x_i-x}{h_x}, \frac{y_i-y}{h_y}\right), \tag{22}$$

where x_i, y_i, for $i = 1, 2, ..., n$ are the samples, h_x, h_y stand for smoothing coefficients. It can be easily deduced from the univariate case.

There are many different multivariate kernels which can be found in applications, e.g., the Epanechnikov kernel:

$$K(u) = \frac{3}{4}(1-u^2), \tag{23}$$

or the Gaussian kernel:

$$K(u) = \frac{1}{\sqrt{2\pi}}e^{-\frac{1}{2}u^2}. \tag{24}$$

From Eq. (22) following estimators are available – the product kernel estimator and the radial kernel estimator.

7. Estimation of Doppler frequency signal scheme

The scheme of the measurement system is shown in Fig. 6.

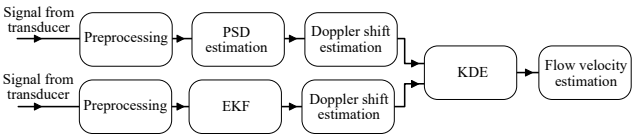

Fig. 6. Signal processing scheme.

The signals from the transducers are first preprocessed for noise cancelation. The PSD estimation is then calculated. When the results obtained from both transducers (oriented in opposite directions) are obtained, the Doppler shift can be determined. Using the KDE approach allows to estimate the fluid flow velocity.

8. Results

The schematic of the measurement system is visible in Figs. 7 and 8. Siemens 191N1S transducers were used with a sampling frequency of 10 MHz and with separate transmit and receive transducers. Such a transducer selection provides the high amount of reflected sound energy with the least synchronous noise from the pipe wall or transducer cross coupling, so this was considered to be the easiest case to prove the principle without any major barriers. The transmitting sine-wave signal was stored in a flash memory and sent to the pipe as a burst every 10 ms. The received signal was amplified by a fixed factor, sampled (16 bits) and sent to the signal processing unit

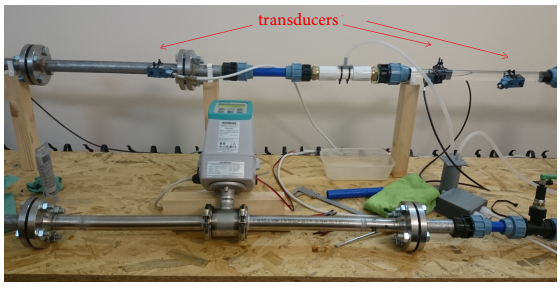

Fig. 7. Measurement equipment.

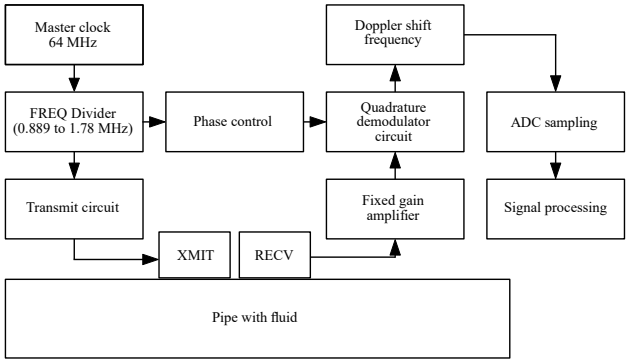

Fig. 8. Measurement system details.

(STM32 processor). Test studies were carried out on an actual system. The test environment consisted of a set of pipes made of PVC, galvanized, and ungalvanized steel. Examples of recorded signals are presented in Fig. 9.

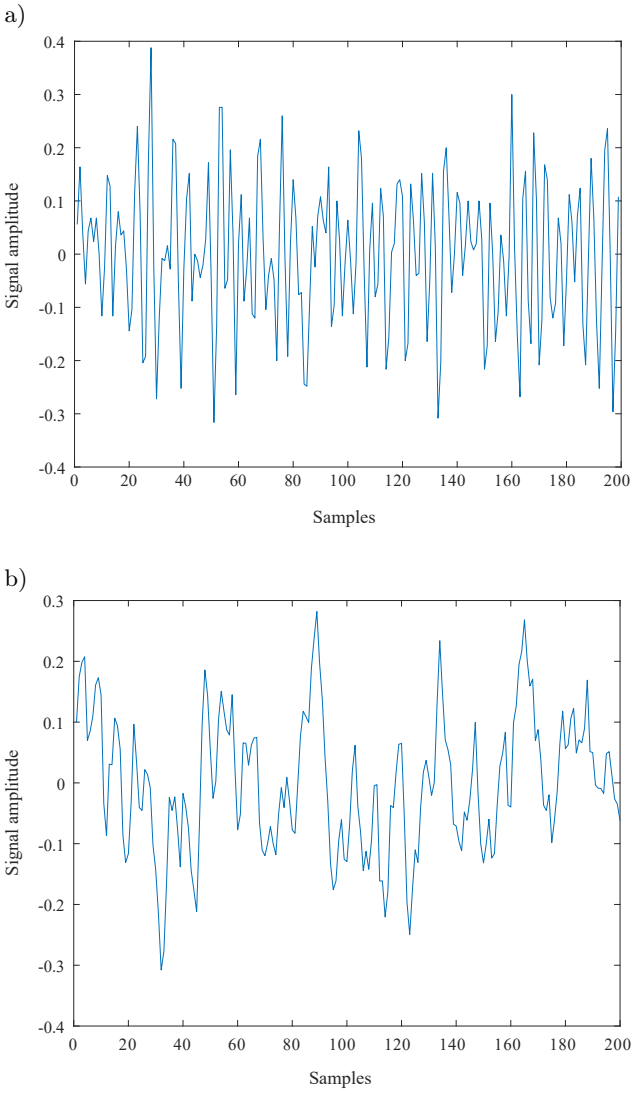

Fig. 9. Examples of the recorded signals:
a) PCV pipe; b) steel galvanized pipe.

Pipes with diameters ranging from 50 mm to 150 mm with closed circulation were used. Measurements were made using air bubbles with a diameter of 1–2 mm. This made it possible to use the pulsed Doppler method. The pump used a guaranteed constant and the same speed of air bubbles and water inside the pipe. Transducers acting as sensors provided measurements for our tests. These were fixed on the horizontal plane. Two transducers measure the Doppler shift – the first measures the negative shift and the second measures the positive shift. It is a result of the fluid velocity. The obtained liquid velocities are presented in Fig. 10.

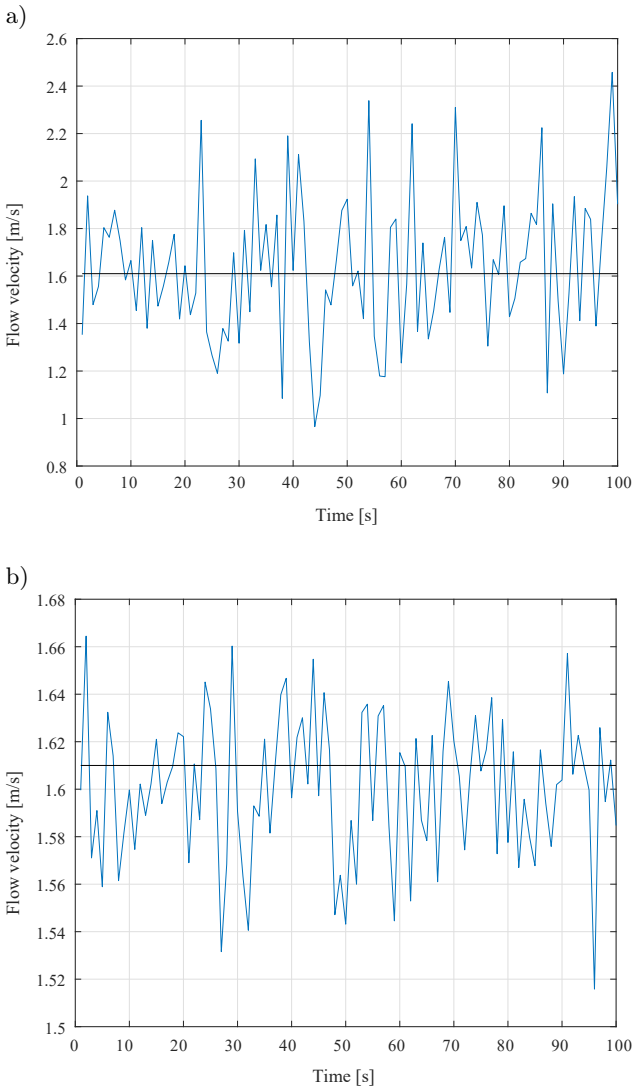

Fig. 10. Obtained liquid velocities:
a) PCV pipe; b) steel galvanized pipe.

The transducers operated at a sampling frequency rate of 10 MHz. The operating signal was a single sine wave with a frequency of 2 MHz and a burst duration of 20 µ. The transmit frequency was equal to 10 kHz. The flow velocity estimated by two methods separately

is presented in Fig. 11 and the accuracy speed liquid for the PCV pipe in Table 1.

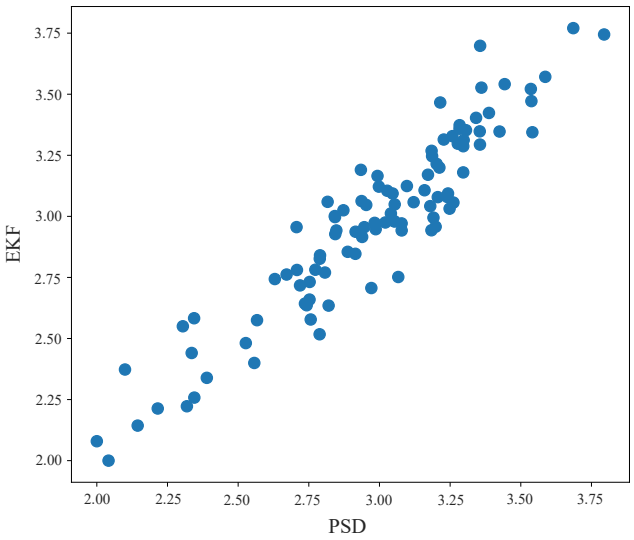

Fig. 11. Flow velocity estimated by two methods separately.

Table 1. Accuracy speed liquid for PCV pipe.

Real flow [m^3/h]	Single method	KDE
0.5	0.6	0.51
1.0	0.94	1.02
1.5	1.40	1.49
2.0	1.92	1.98
2.5	2.53	2.51
3.0	3.10	2.98

8.1. Comparison of fluid velocity estimation results for the analysed PSD estimators

PSD were estimated with two non-parametric methods: MTM and Welsh algorithms and two parametric: Burg and Prony methods. Different cases were analysed: positive and negative flow, different liquid flow velocity, different pipe diameters, and different pipe material. The mean flow velocity of the liquid estimation results for each of the four estimators of the PSD is shown in Table 2.

Table 2. Accuracy speed liquid for PSD pipe.

Pipe number	Real flow	Burg	Prony	MTM	Welch
1	0.20	0.2120	0.51	0.2202	0.2374
2	0.21	0.2099	0.4277	0.2126	0.1968
3	0.66	0.6639	1.2993	0.5740	0.6321
4	0.65	0.6776	1.3036	0.5898	0.6126
5	0.21	0.2162	1.0013	0.2189	0.2009

For each power spectral density estimator, the relative error between the exact value of the liquid flow velocity and the measured value was calculated. Errors are expressed as a percentage and results are shown in Fig. 12. It follows from Fig. 12 and Table 2 that the estimation of the power spectral density using the parametric Burg method had the smallest errors. To maintain the legibility of the above figure, the relative values of errors using the parametric Prony method were not included, as the errors reached several hundred percent.

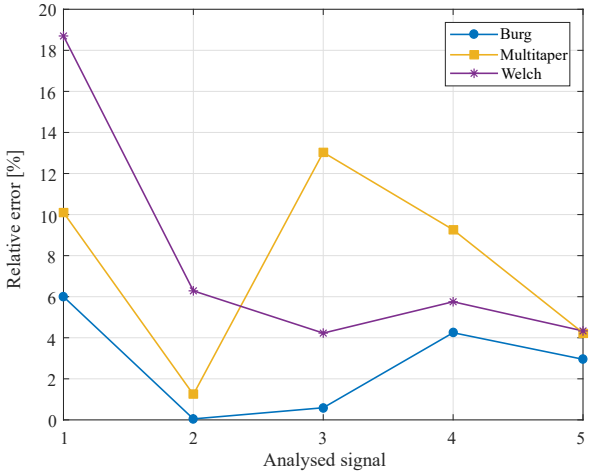

Fig. 12. Relative error plot of liquid flow velocity estimation for four power spectral density estimators.

After averaging the results, the global error was determined for each of the estimators. The results are presented in Table 3.

Table 3. Global error [%].

Burg	Prony	MTM	Welch
2.77	166.58	7.58	7.86

Figure 13 shows the variance of the power spectral density estimators used, for each of the analysed pipes in which fluid flow was studied. It is clear from

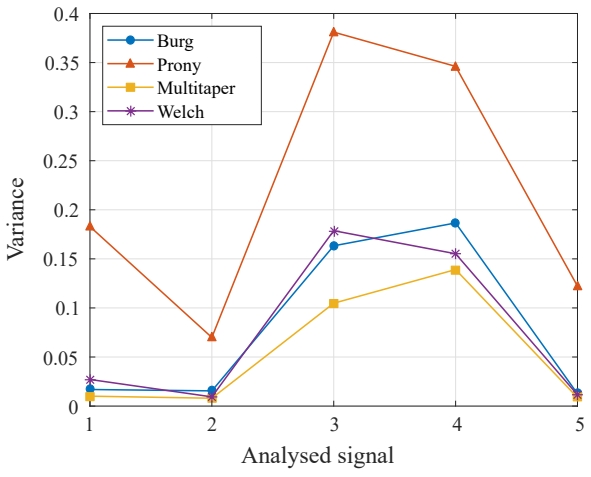

Fig. 13. The variance of the PSD estimators.

Fig. 13 above that the non-parametric MTM estimator has the smallest variance. Similar to the error analysis, the parametric Prony estimator has the highest variance.

9. Conclusions

The methods used to combine measurements for non-invasive measurement of the fluid flow velocity have proven to be accurate and return correct values. This has the advantage of using algorithms with low computational complexity. In combination with the KDE approach, a convenient and accurate tool was obtained. Another advantage of this solution is the ease of mounting the sensors in the pipe. A measurement accuracy of >95% was obtained.

References

1. Atkins M.D. (2016), Velocity field measurement using particle image velocimetry (PIV), [in:] *Application of Thermo-Fluidic Measurement Techniques*, Kim T., Lu T.J., Song S.J. [Eds.], pp. 125–166, doi: 10.1016/B978-0-12-809731-1.00005-8.
2. Avilán E.J., Reis V., Barreira L.E., Salgado C.M. (2013), Evaluation of cross correlation technique to measure flow in pipes of the oil industry, [in:] *2013 International Nuclear Atlantic Conference – INAC 2013*.
3. Bar-Shalom Y., Li X.-Rong, Kirubarajan T. (2004), *Estimation with Applications to Tracking and Navigation: Theory, Algorithms and Software*, John Wiley & Sons.
4. Beck M.S., Plaskowski A. (1987), *Cross Correlation Flowmeters, Their Design and Application*, Taylor & Francis.
5. Buermans J., Lampa J., Lemon D. (2009), Turbine flow measurement in low-head plants – Acoustic scintillation flow meter: Why? How? Where?, *Medicine*, Corpus ID: 113046881.
6. Cochran S. (2001), Ultrasonic instruments & devices – reference for modern instrumentation, techniques and technology, *Ultrasound in Medicine and Biology*, **27**(10): 1439, doi: 10.1016/S0301-5629(01)00386-6.
7. Cui Z. *et al.* (2016), A review on image reconstruction algorithms for electrical capacitance/resistance tomography, *Sensor Review*, **36**(4): 429–445, doi: 10.1108/SR-01-2016-0027.
8. Doran P.M. (2013), *Bioprocess engineering principles*, 2n ed., Academic Press Waltham.
9. Grewal M.S., Andrews A.P. (2001), *Kalman Filtering: Theory and Practice Using MATLAB*, 2nd ed., John Wiley & Sons.
10. Jazwinski A.H. (1970), *Stochastic Processes and Filtering Theory*, Elsevier Science.
11. Jones F.E (1995), *Techniques and topics in flow measurement*, CRC Press.
12. Kaipio J.P. *et al.* (2015), Process tomography and estimation of velocity fields, [in:] *Industrial Tomography*, Wang M. [Ed.], pp. 551–590, Woodhead Publishing, doi: 10.1016/B978-1-78242-118-4.00021-6.
13. Kang L. *et al.* (2019), Flow velocity measurement using a spatial averaging method with two-dimensional flexural ultrasonic array technology, *Sensors*, **19**(21): 4786, doi: 10.3390/s19214786.
14. Lucas G.P., Cory J., Waterfall R.C., Loh W.W., Dickin F.J. (1999), Measurement of the solids volume fraction and velocity distributions in solids-liquid flows using dual-plane electrical resistance tomography, *Flow Measurement and Instrumentation*, **10**(4): 249–258, doi: 10.1016/S0955-5986(99)00010-2.
15. Lyons R. (2004), *Understanding Digital Signal Processing*, 2nd ed., Pearson Education Incorporated.
16. Maybeck P.S. (1982), *Stochastic Models, Estimation and Control: Volume 2*, Academic Press.
17. Matani A., Oshiro O., Chihara K. (1996), Doppler signal processing of blood flow using a wavelet transform, *Japanese Journal of Applied Physics*, **35**(5S), doi: 10.1143/jjap.35.3131.
18. Mori M., Tezuka K., Aritomi M., Kukura H., Takeda Y. (2004), Industrial application experiences of new type flow-metering system based on ultrasonic-Doppler flow velocity-profile measurement, [in:] *Fourth International Symposium on Ultrasonic Doppler Methods for Fluid Mechanics and Fluid Engineering*, Japan.
19. Raffel M., Willert C.E., Kompenhans J. (1998), *Particle Image Velocimetry: A Practical Guide*, Springer Berlin, doi: 10.1007/978-3-662-03637-2.
20. Särkkä S. (2006), *Recursive Bayesian Inference on Stochastic Differential Equations*, Helsinki University of Technology, Laboratory of Computational Engineering Publications, Report B54, ISBN: 951-22-8127-9.
21. Solero G., Beghi M. (1995), Experimental fluid dynamic characterization of a premixed natural gas burner for domestic and semi-industrial applications, [in:] *The Institute of Energy's Second International Conference on Combustion & Emissions Control*, pp. 39–48, doi: 10.1016/B978-0-902597-49-5.50007-X.
22. Takeda Y. (1995), Instantaneous velocity profile measurement by ultrasonic Doppler method, *JSME International Journal Series B Fluids and Thermal Engineering*, **38**(1): 8–16, doi: 10.1299/jsmeb.38.8.
23. Takeda Y. (2012), *Ultrasonic Doppler Velocity Profiler for Fluid Flow, Fluid Mechanics and its Applications*, Springer, ISBN: 978-4-431-54026-7.
24. Xu Y., Wang H., Cui Z., Dong F. (2009), Application of electrical resistance tomography for slug flow measurement in gas/liquid flow of horizontal pipe, [in:] *2009 IEEE International Workshop on Imaging Systems and Techniques*, pp. 319–323, doi: 10.1109/IST.2009.5071657.
25. Wu J. (2018), Acoustic streaming and its applications, *Fluids*, **3**(4): 108, doi: 10.3390/fluids3040108.